

Magnetic coupling in granular aluminum superconducting films

K. E. Gray

Materials Science and Technology Division, Argonne National Laboratory, Argonne, Illinois 60439

(Received 8 December 1982)

The maximum coupling force F_{cm} in a Giaever superconducting transformer is measured in granular aluminum films at significantly higher fields and lower temperatures than in previous work. A new method to determine F_{cm} by measuring the critical current in one film only is presented. The results are in excellent quantitative agreement with the one-reciprocal-lattice-vector approximation to the theoretical analysis in its region of validity, i.e., at high fields. For low fields, F_{cm} is consistent with the temperature dependence of the low-field approximation over the entire reduced-temperature ($t = T/T_c$) range ($0.36 < t < 0.96$).

I. INTRODUCTION

The study of magnetic coupling of thin type-II superconducting films began with the ingenious experiments of Giaever.¹ In these experiments a magnetic field is applied perpendicular to two superconducting films, one laying on top of the other. Flux vortices of one flux quantum each then thread both films. Even when the films are electrically insulated, a current in one film only, which causes flux flow, can induce a voltage in the second film if the force coupling the vortices in each film is stronger than the pinning forces.

When it was shown² that granular aluminum films can exhibit extremely low flux pinning, studies shifted to this material. Measurements in low fields^{3,4} near the superconducting transition temperature T_c were shown to be in excellent quantitative agreement with theoretical calculations.^{5,6} In these experiments, the current-voltage characteristics of one film were measured as a function of the current in the other film. Prominent features in these curves were used to deduce the maximum coupling force.

It is the purpose of this paper to extend these measurements to much lower temperatures and higher fields. In doing so, a new method is introduced to determine the coupling force from critical-current measurements of one film alone. At very low fields, coupling is hard to observe by traditional methods^{1,3} because the flux lines are weakly bound in a lattice and the pinning force is high. At high fields, the coupling force is much less than the pinning force, so the traditional method lacks resolution. However, this new method is only useful when the pinning is much stronger in one of the two films.

An important result is that the coupling force appears to diminish very rapidly for fields of only about one-third of the critical field. However, in addition, it is demonstrated for the first time that the simplifying one-reciprocal-lattice-vector approximation^{3,4,6} is valid for high fields. In fact, this assumption seems to give the same excellent quantitative agreement over the extended temperature and field ranges as the complete theory^{4,6} does for low fields.

Studies of magnetic coupling in thin films may shed light on the important problems of flux flow in technological superconductors, including the question of the sum-

mation of pinning forces⁷ and possible limited usefulness of strong pinning centers due to flux cutting.⁸

II. SAMPLE PREPARATION AND CHARACTERIZATION

Our samples consisted of two granular aluminum films of width $w = 1.5$ mm and thickness $d_f = 1000$ Å, which were reactively evaporated at a rate of about 10 Å/sec in an oxygen-rich atmosphere of total pressure $\sim 1.3 \times 10^{-5}$ Torr. Both films were condensed through an H -pattern mask so that four-terminal current-voltage characteristics $I(V)$ could be measured. The first film was considerably longer and extended beyond the ends of the second short film (see inset of Fig. 1). Insulation was provided by oxidizing the first film for \sim one day in wet air. This resulted in a high-quality tunnel junction (low leakage current) of specific resistance ~ 65 Ω cm². The large junction

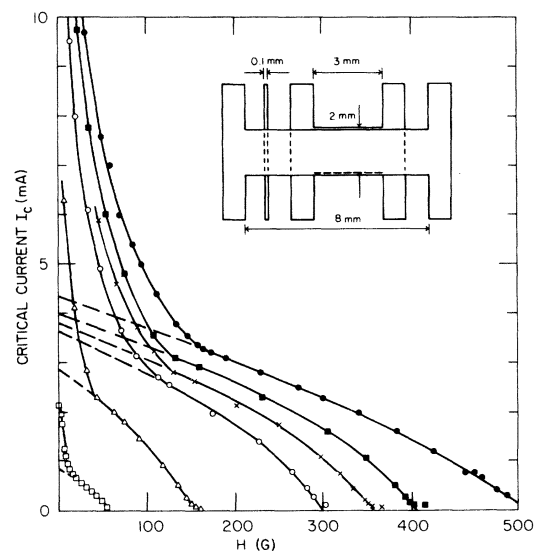


FIG. 1. Critical current for the short film as a function of magnetic field and reduced temperature. The dashed line extrapolations of the high-field behavior is explained in the text. Reduced temperatures are: ● 0.36; ■ 0.52; × 0.59; ○ 0.66; △ 0.81; □ 0.93. Inset: geometry of sample, the exaggerated misalignment is actually negligible.

specific resistance relative to the resistance per square of the film $\rho_n/d_f \cong 0.84 \Omega$ ensured that leakage currents did not affect critical current nor resistance measurements. The measured normal-state resistivities ρ_n were reduced due to the second film by 1 part in 10^4 .

For the long and short films, ρ_n was 8.4 and 8.5 $\mu\Omega$ cm, respectively. Using the average of these, the Ginzburg-Landau parameter κ is given by Ref. 9 to be 2.29. The transition temperatures of the films were $T_c \cong 1.53$ K. Tunneling measurements showed the energy gaps of the films to be sharp [$\delta\Delta(0)/\Delta(0) \sim 3\%$] and nearly equal with a low-temperature value of $\Delta(0) \cong 230 \mu\text{V} \cong 1.75kT_c$. The critical field $B_{c2}(t)$ determined from the tunnel junction characteristic and by extrapolating the critical current I_c for each film agreed⁹ within experimental error and was well represented by

$$B_{c2}(t) = B_{c2}(0)(1-t) \quad (1)$$

for $t \geq 0.5$, where $B_{c2}(0) \cong 768$ G. (The field was applied by a long solenoid which was calibrated by a Hall probe. Samples were mounted in a standard He³ cryostat using carbon resistance thermometry.)

III. COUPLING FORCE MEASUREMENTS

For samples of the type described in the preceding section, the critical currents (I_c) have been measured for each film *individually*, as a function of perpendicular magnetic field (B) and reduced temperature ($t = T/T_c$). The critical current was defined by the current at which 1 μV appeared across the sample. The results for the short film, with no external current flowing through the long film, are shown in Fig. 1. There seems to be an abrupt change of behavior at $B \sim B_{c2}/3$ at each temperature. The results for the longer film were significantly different: Although the shapes of I_c vs B for the long and short films were the same at high fields, the magnitude of I_c in the long film was larger (up to 8 times at low temperatures), indicating much stronger pinning, and the high-field behavior persisted to much lower fields (5–10% of B_{c2}) below which I_c increased more rapidly. There does not seem to be any explanation of this uncommon difference in I_c for otherwise similar films. (The dependence of I_c on resistivity for most of our samples agreed with the earlier work.²)

When appropriate currents were applied to sets of films of this type, the voltages displayed the usual behavior associated with magnetic coupling.^{3,5} This leads one to interpret the difference in the field dependence of I_c for these two films in terms of magnetic coupling, and in doing so, to find a new experimental method to determine the maximum coupling force F_{cm} .

To understand how magnetic coupling can explain the difference in I_c , first note that in a *static* situation at I_c , both F_{cm} and the pinning force act opposite to the Lorentz force. Thus F_{cm} can only increase I_c above its intrinsic value (without coupling). As a result, it is the intrinsic I_c which is measured in the long film since there is a section without overlap; however, I_c in the short film will be increased by any contributions due to coupling.

Because the intrinsic pinning force (i.e., I_c) is significantly greater in the long film, the vortices, which necessarily thread both films, are stationary (pinned) in the long

film even when they move in the short film ($I > I_c$ of Fig. 1). As a result, the I_c of the short film represents the sum of its intrinsic pinning force plus the maximum coupling force F_{cm} (provided F_{cm} is less than the pinning force in the long film). Thus F_{cm} can be evaluated if the intrinsic I_c is known.

To find this, a reasonable extrapolation of the high field I_c is made (dashed lines of Fig. 1) using an initial justification the similar behavior of the intrinsic I_c of the long film. On the other hand, at very low fields, even the intrinsic long film I_c increases above its high-field extrapolation. This is presumably due to the breakup of a rigid flux-line lattice (FLL) so that individual flux lines can find the strongest pinning centers.⁷ However, in the absence of a rigid FLL the flux-line positions in the weaker pinning short film will be determined by the stronger pinning centers in the long film. Thus, because of the coupling, the strongest pinning centers of the short film are not necessarily occupied, and the dashed curve shown in Fig. 1 may be valid down to the lowest measured fields (~ 0.3 G). Evidence that this is approximately valid can be found in the following analysis of the low-field measurements.

The theoretical model for magnetic coupling⁵ predicts that F_{cm} in the limit of zero field is given by

$$F_{cm} = \phi_0^2 / 8\pi^2 \rho_{\text{eff}}^2, \quad (2)$$

where ϕ_0 is the flux quantum and

$$\rho_{\text{eff}} = d_i + 2\lambda \coth(d_f/\lambda). \quad (3)$$

In Eq. (3), equal film thicknesses d_f and penetration depths λ are assumed, and d_i is the insulator thickness between the two films (d_i is not known but is of order 50 $\text{\AA} \ll d_f, \lambda$). Presupposing the conclusion that $\lambda \gg d_f$, Eq. (2) becomes

$$F_{cm} = \phi_0^2 d_f^2 / 32\pi^2 \lambda^4 (t). \quad (4)$$

To verify Eq. (4), the phenomenological temperature dependence of the weak-field penetration depth is used,¹⁰

$$(\lambda_0/\lambda)^2 = (1-t^4), \quad (5)$$

where λ_0 is the zero-temperature penetration depth, together with³

$$F_{cm} = \phi_0 I_0 / cw, \quad (6)$$

where I_0 is the measured I_c of the short film, minus the high-field extrapolation, c is the velocity of light, and w is the film width. These low-field data are shown in Fig. 2 as the black squares and thus verify Eq. (4). The use of Eq. (4) is verified by noting that the straight line is for $\lambda_0 \approx 3500 \text{\AA} \gg d_f = 1000 \text{\AA}$.

IV. COMPARISON WITH THEORY

The success of the theory in explaining the low-field results over the entire temperature range encourages one to consider the high-field limit as well, to see, for example, if the rapid decrease in F_{cm} for $B \gtrsim B_{c2}/3$ is predicted. The extension⁶ of the theory to large B requires a significant modification of Eq. (4). However, a considerable simplification occurs for B greater than

$$B_t \cong \phi_0 / (32\sqrt{3})\lambda^2. \quad (7)$$

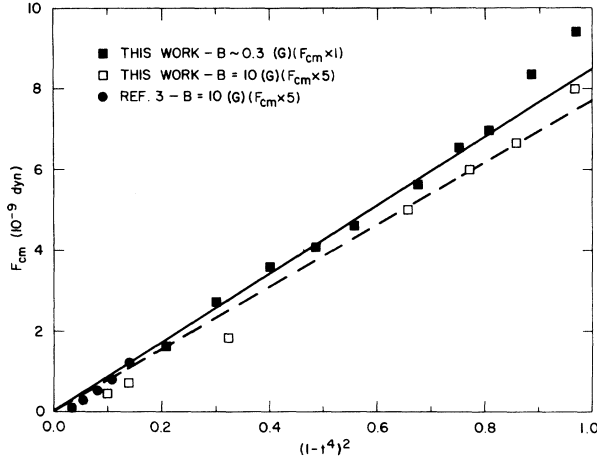


FIG. 2. Maximum coupling force vs a function of reduced temperature for low fields (■) and for 10 G (□—our data; ●—data of Ref. 3). The 10-G data are plotted 5 times larger than the actual values.

Note that B_t must be determined self-consistently since λ depends on B through⁴

$$(\lambda_0/\lambda)^2 = (1-t^4) \left[1 - \frac{B}{2B_{c2}(t) - B} \right]. \quad (8)$$

For the films reported here, B_t ranges from about 16 G at low t to 2.5 G at $t=0.95$.

It is again assumed that the films are identical, $\lambda \gg d_f$, and also that $B \gg B_t$, and the vortex core parameter¹¹ $\xi_v \ll \lambda$. Then the so-called one-reciprocal-lattice-vector approximation^{3,4,6} (ORLVA) should be valid:

$$F_{cm} \cong F_0 (1 - e^{-g_{10} d_f})^2 e^{-g_{10} d_i} (g_{10} \xi_v)^2 \times K_1^2 (g_{10} \xi_v) (\lambda_0/\lambda)^4 / g_{10}^2 d_f^2, \quad (9)$$

where $F_0 = 3\phi_0^2 d_f^2 / 32\pi^3 \lambda_0^4$, the shortest reciprocal-lattice vector $g_{10} = (8\pi^2 B / \sqrt{3}\phi_0)^{1/2}$, and K_1 is a modified Bessel function. Clem¹¹ has calculated ξ_v/ξ_{GL} , where ξ_{GL} is the Ginzburg-Landau (GL) coherence length, to be a weak function of the GL parameter κ and approximately equal to unity. Since all of the data going into Eq. (9) can be measured independently, we proceed with a *no*-parameter comparison of experiment [Eq. (6)] and theory [Eq. (9)].

The critical field [Eq. (1)] determines ξ_{GL} through the usual GL relation¹⁰

$$\xi_{GL}^2(t) = \phi_0 / 2\pi B_{c2}(t), \quad (10)$$

but also κ , since near T_c one finds⁹

$$\kappa = B_{c2}(t) / \sqrt{2} B_{cb}(t), \quad (11)$$

where $B_{cb}(t)$ is the critical field of bulk type-I aluminum.¹² Now from the definition $\kappa \equiv \lambda/\xi$, it is found that near T_c

$$\lambda_0^2 = 2\phi_0 \kappa^2 (1-t) / \pi B_{c2}(t). \quad (12)$$

Evaluating these equations results in $\xi_{GL}(1-t)^{1/2} \cong 660 \text{ \AA}$, $\kappa = 2.29$ in agreement with the previous determination from ρ_n , $\lambda_0 = 2950 \text{ \AA}$, and¹¹ $\xi_v \cong 1.17 \xi_{GL}$.

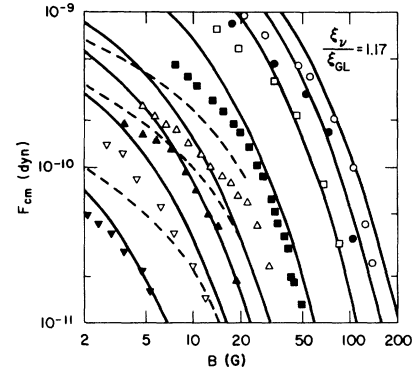


FIG. 3. Maximum coupling force vs field for various reduced temperatures (○ 0.36; ● 0.52; □ 0.66; ■ 0.81; △ 0.89; ▲ 0.91; ▽ 0.93; ▼ 0.96). The data for $B < B_t$ are not shown. The solid lines are calculations using the ORLVA and *no* adjustable parameters. The dashed lines are the data of Ref. 3 for $t=0.89, 0.92$, and 0.95 from top to bottom.

The evaluation of Eq. (9) using these parameter values and Eq. (6) using the experimental data of Fig. 1 results in Fig. 3. In spite of some disagreement, the overall correspondence of magnitude as well as field and temperature dependence is quite encouraging, especially considering that *no* adjustable parameters were used. Note that data below $\sim B_t$ are not shown.

The fact that the experimental data tend to fall below theory at small fields is puzzling at first sight, since (a) the correct intrinsic I_c may be larger than the dashed line of Fig. 1, leading to an even smaller experimental F_{cm} and (b) the comparison of Ref. 6 of the ORLVA with the exact result indicates the calculated F_{cm} should be even larger for $B \leq B_t$. Notice that this tendency persists to lower fields: The low-field data of Fig. 2 were fitted using a *larger* λ_0 than that used in Fig. 3. However, Fig. 2 also shows F_{cm} at 10 G (open squares) to be in good agreement with Eqs. (4) and (5) at low t (where $B < B_t$), underlining agreement with the general features of the theory.

A possible explanation of this low-field behavior (with little justification) is that the weakened FLL for $B < B_t$ leads to a *lower intrinsic* I_c in the short film because the flux-line locations are determined by the stronger pinning, long film through the coupling force. A second possible explanation is that the intrinsic pinning force in the long film is smaller than the maximum coupling force. This, however, is not borne out by direct measurements of I_c in the long film at low t and intermediate fields where the effect is also significant.

Such explanations, as well as the general features of the coupling, could give insight into the important practical problems of flux pinning in technological superconductors (i.e., the question of the summation of pinning forces,⁷ flux cutting which limits the usefulness of strong pinning centers,⁸ etc.).

The value obtained for ξ_{GL} is in excellent agreement with a simple determination based on the theory of dirty superconductivity. Following Ref. 4, we find the following: $\xi_0 \cong 12500 \text{ \AA}$, the electron mean free path¹³ is $\hat{l} \cong 47 \text{ \AA}$, and therefore $\xi_{GL}(0) = 0.85(\xi_0 \hat{l})^{1/2} = 650 \text{ \AA}$ in excellent agreement with 660 \AA found from Eq. (10). However, the comparison is not as good for λ_0 : Using the London

penetration depth for bulk aluminum $\lambda_L(0)=157 \text{ \AA}$, we find $\lambda_0 \cong 0.61\lambda_L(0)(\xi_0/\hat{l})^{1/2} \cong 1560 \text{ \AA}$, which is substantially less than the value of 2950 \AA used in the fit of Fig. 3. The bulk $\lambda_L(0)$ is expected to be valid because specific-heat measurements¹⁴ on granular aluminum show the same density of electron states at the Fermi energy as bulk. The resolution of this discrepancy may be related to the granular structure of these films, since λ involves currents flowing from grain to grain whereas the specific heat does not. For example, if oxides occur in the grain boundaries, the resulting poorer coupling may increase the effective $\lambda_L(0)$.

It should be pointed out that a very acceptable fit of the F_{cm} data to theory can be obtained by a different set of parameter values. An example is shown in Fig. 4, in which the shapes of the curves are changed by using $\xi_v/\xi_{GL}=0.8$ rather than Clem's value¹¹ of 1.17. As a result, we must use $\lambda_0=3880 \text{ \AA}$ rather than the calculated value from ξ_{GL} and κ of 2950 \AA . Thus one is faced with a certain ambiguity; however, the solution using no adjustable parameters must be considered superior unless contrary evidence about ξ_v is obtained in future experiments.

V. COMPARISON WITH OTHER EXPERIMENTS

Experiments on very similar films have been reported in Ref. 3 and further analyzed in Ref. 4 as the "thin film" example. The properties of both films were very similar, and their following *average values* should be compared to those for our films (Sec. II). They find $d_f=750 \text{ \AA}$, $\rho_n \cong 8.7 \mu\Omega \text{ cm}$, $T_c \cong 1.54 \text{ K}$, and $d_i=120 \text{ \AA}$. They have also determined from these that $\xi_{GL}(0) \cong 640 \text{ \AA}$, and using Ref. 9, we find $\kappa \cong 2.34$. Thus their measurements of F_{cm} are expected to be, and are, very close to ours. When the data of Ref. 3 are plotted (as dashed curves) with our data in Fig. 3, the trends are similar; however, our data are about 40% smaller for a given t and fall off more rapidly as $B \rightarrow 10 \text{ G}$. This more rapid drop-off of F_{cm} around 10 G at high t is also shown in Fig. 2; but note that at high t , $B=10 \text{ G} \geq B_t$, so Eq. (4) is not expected to be valid and therefore our data should drop below the dashed line in Fig. 2.

The authors of Ref. 4 have fitted their F_{cm} data using the exact theory (without the ORLVA) because the field strengths are approximately equal to B_t . Rather than fixing λ_0 in Eq. (8) from κ and ξ_{GL} , they have determined $\lambda(B,t)$ for each data point. They find good agreement with Eq. (8) for the field dependence and arrive at a value of $\lambda_0=3260 \text{ \AA}$. This is to be compared directly to our determination of 2950 \AA since the products of $\kappa\xi_{GL}$ for the two samples are essentially identical. This small discrepancy is certainly within the limits of the fitting procedure, since we have shown in Fig. 4 another reasonable fit using $\lambda_0=3880 \text{ \AA}$.

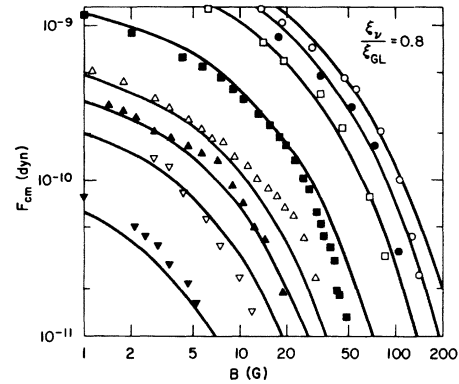


FIG. 4. Same data and symbol notation of Fig. 3, but the calculations assume the smaller core parameter $\xi_v/\xi_{GL}=0.8$ rather than the 1.17 predicted by Ref. 11 and used in Fig. 3.

The final resolution of the small numerical discrepancies may be rooted in the homogeneity of the films used in these studies. Because the reactive evaporation used to make the samples is unstable against fluctuations in oxygen pressure and evaporation rate, significant deviations in oxygen content, and hence ρ_n , may occur through the thickness of the film.

The fact that our F_{cm} drops off somewhat more rapidly at high field ($\sim 10 \text{ G}$) than in Ref. 3 is also somewhat disturbing. For higher fields, both our extrapolation for the intrinsic I_c and the ORLVA should be best. However, these details are perhaps less important than the overall correspondence with theory. Our results at lower t and higher fields add greatly to this already impressive agreement and show for the first time that the ORLVA is essentially correct.

VI. CONCLUSIONS

The results of magnetic coupling are extended to a much wider range of temperatures and fields. The limiting approximations of the theory at low and high field are verified for the first time, and also in the case of high fields with no adjustable parameters. This overall agreement is also extended to a much wider range of temperatures and complements the previous experimental results.^{3,4}

ACKNOWLEDGMENT

This work was supported by the U.S. Department of Energy.

¹I. Giaever, Phys. Rev. Lett. **15**, 825 (1966); **16**, 460 (1966).

²J. W. Ekin, Phys. Rev. B **12**, 2676 (1975).

³J. W. Ekin, B. Serin, and John R. Clem, Phys. Rev. B **2**, 912 (1974).

⁴J. W. Ekin and John R. Clem, Phys. Rev. B **12**, 1753 (1975).

⁵John R. Clem, Phys. Rev. B **2**, 898 (1974).

⁶John R. Clem, Phys. Rev. B **12**, 1742 (1975).

⁷A. M. Campbell and J. E. Evetts, *Critical Currents in Supercon-*

ductors (Taylor and Francis, London, 1972); Adv. Phys. **21**, 199 (1972); H. Ullmaier, *Irreversible Properties of Type II Superconductors* (Springer, Berlin, 1975).

⁸D. G. Walmsley, J. Phys. F **2**, 510 (1972); J. R. Clem, Phys. Rev. Lett. **38**, 1425 (1977).

⁹K. E. Gray, Phys. Rev. B **13**, 3774 (1976).

¹⁰M. Tinkham, *Introduction to Superconductivity* (McGraw-Hill, New York, 1975).

¹¹John R. Clem, J. Low Temp. Phys. 18, 427 (1975).

¹²E. P. Harris and D. E. Mapother, Phys. Rev. 165, 522 (1968).

¹³T. E. Faber and A. B. Pippard, Proc. R. Soc. London Ser. A

231, 366 (1955).

¹⁴R. L. Greene, C. N. King, R. B. Zubeck, and J. J. Hauser, Phys. Rev. B 6, 3297 (1972).